Structural Response and Energy Absorption of Sandwich Panels with an Aluminium Foam Core Under Blast Loading

Feng Zhu[1], Longmao Zhao[1,2], Guoxing Lu[1,3,*] and Zhihua Wang[1,2]

[1]Faculty of Engineering and Industrial Sciences, Swinburne University of Technology, Australia
[2]Institute of Applied Mechanics and Biomedical Engineering, Taiyuan University of Technology, PR China
[3]School of Mechanical and Aerospace Engineering, Nanyang Technological University, Singapore

(Received: 1 February 2008; Received revised form: 7 August 2008; Accepted: 9 August 2008)

Abstract: This paper first presents an experimental investigation into the response of square sandwich panels with an aluminium foam core under blast loading, followed by a corresponding FE simulation using LS-DYNA. In the simulation, the loading process of explosive and response of the sandwich panels have been investigated. The blast loading process includes both the explosion procedure of the charge and interaction with the panel. The simulation result shows that the deformation/failure patterns observed in the tests are well captured by the numerical model, and quantitatively a reasonable agreement has been obtained between the simulation and experiment. Finally, a parametric study has been carried out to investigate the energy absorption performance of sandwich panels.

Key words: sandwich panel, aluminium foam, blast loading, FE simulation, energy absorption.

1. INTRODUCTION

Sandwich panels with a cellular core such as metal foams (frequently aluminium foams) have the capability of dissipating considerable energy by large plastic deformation under static or dynamic loading. The cellular microstructures offer them with the ability to undergo large plastic deformation at nearly constant nominal stress, and thus can absorb a large amount of kinetic energy before collapsing to a more stable configuration or fracture (Ashby *et al*. 2000; Gibson and Ashby 1997; Lu and Yu 2003). In recent years, increasing attention of both engineering communities and government agencies has been paid to their responses subjected to blasts, due to enhanced chance of blast threats by accidents or terrorist attacks. To date, research on the behaviour of blast loaded sandwich structures is still very limited. Although some studies have been conducted on sandwich beams and circular sandwich panels (Fleck and Deshpande 2004; Qiu *et al*. 2003, 2004; Xue and Hutchinson 2003) and square panels with conventional honeycomb core (Zhu et al. 2008), either experimental investigations or numerical simulations on square sandwich panels with metallic foam core have yet to be reported.

In this research, systematic investigations were carried out experimentally and computationally into square sandwich panels with aluminium foam as core. The experimental details and results are described in Section 2. Based on the experiments, corresponding finite element simulations were conducted using LS-DYNA, and the simulation results are presented and analyzed in Section 3. In the simulations, the process of blast loading and response of sandwich panels are investigated. The blast loading process includes a detonation stage of charge as well as its interaction with

*Corresponding author. Email address: gxlu@ntu.edu.sg.

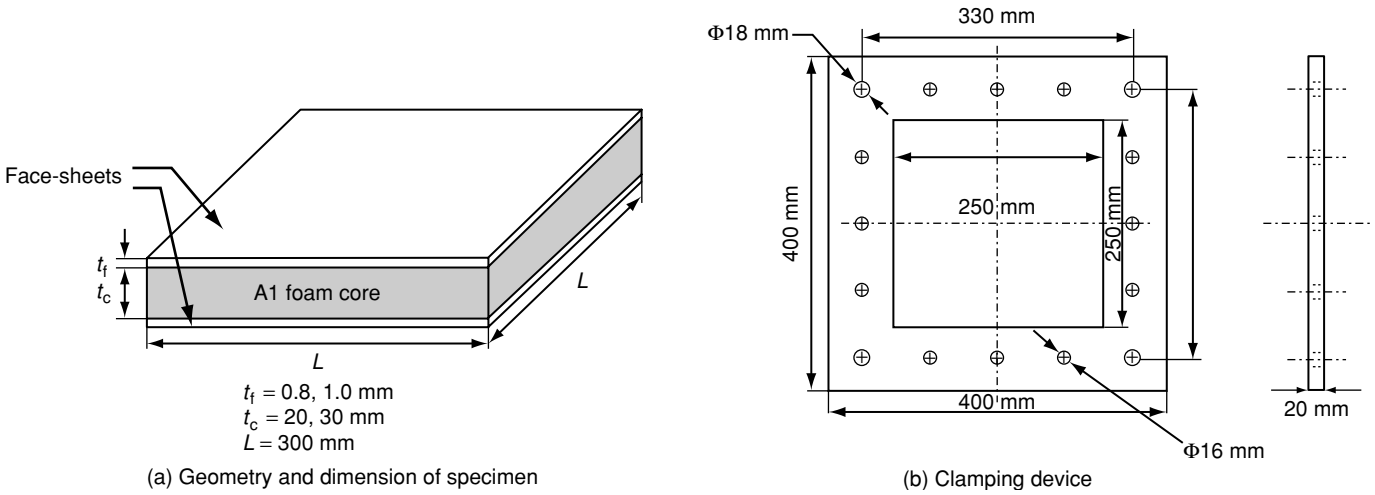

Figure 1. Specimen and clamping device

Table 1. Specifications of the sandwich panels and experimental results

No. of specimen	Name of specimen	Face-sheets thickness t_f (mm)	Mass of core m_o (g)	Relative density (%)	Core thickness t_c (mm)	Mass of charge m_t (g)	Impulse I (Ns)	Back face deflection w_0 (mm)	Front face tearing
1	L-20-TK-1	1.0	290	6.0	20	20	18.29	4.9	No
2	L-20-TK-2	1.0	292	6.1	20	30	22.57	6.1	No
3	H-20-TK-1	1.0	466	9.7	20	20	18.08	4.4	No
4	H-20-TK-2	1.0	472	9.8	20	30	23.00	5.1	No
5	L-30-MD-1	0.8	460	6.4	30	30	22.67	6.2	No
6	L-30-MD-2	0.8	458	6.3	30	40	—	6.3	Yes
7	L-30-TK-1	1.0	461	6.4	30	30	22.32	5.6	No
8	L-30-TK-2	1.0	461	6.4	30	40	25.85	7.0	No
9	H-30-TK-1	1.0	728	10.1	30	30	22.36	2.4	No
10	H-30-TK-2	1.0	714	9.9	30	40	25.55	3.9	No

the panel. The structural response of sandwich panels is investigated in terms of both the deformation/failure patterns of specimens as observed in the tests; and quantitative assessment, which is related to the permanent central point deflection of back face. Finally in Section 4, a parametric study is carried out to examine the energy dissipating history of the sandwich panel, as well as the partition of the plastic energy absorbed by different component parts of the panels; the effect of panel configurations is also analysed.

2. EXPERIMENT

2.1. Specimen

The specimens used in the tests consisted of two identical face-sheets and a core of aluminium foam, as shown in Figure 1(a). The face-sheets were made of aluminium alloy 2024-T3 and had two different thicknesses i.e. MD (t_f = 0.8mm) and TK (t_f = 1.0mm), respectively. The aluminium foam cores had two relative densities, that is 6% (denoted L) and 10% (denoted H). The cores were cut into 300mm × 300mm plates with two different thicknesses (t_c = 20mm and 30mm). Specifications of the plates are presented in Table 1. The panels were peripherally clamped between two square steel frames, as shown in Figure 1(b).

2.2. Set-Up

A four-cable ballistic pendulum system has been employed to measure the impulse delivered on the pendulum/specimen. Figure 2 shows the pendulum set-up. The frames were clamped on the front face of the pendulum, and the charge was fixed in front of the centre of the specimen using an iron wire with a constant stand-off distance of 200mm. With a TNT charge detonated in front of the pendulum face, the impulsive load produced by explosion would push the pendulum to translate. Based on the oscillation amplitude measured by a laser displacement transducer, the impulse transfer was further estimated. Another sensor, known as PVDF pressure gauge was mounted at the centre of the specimen's front

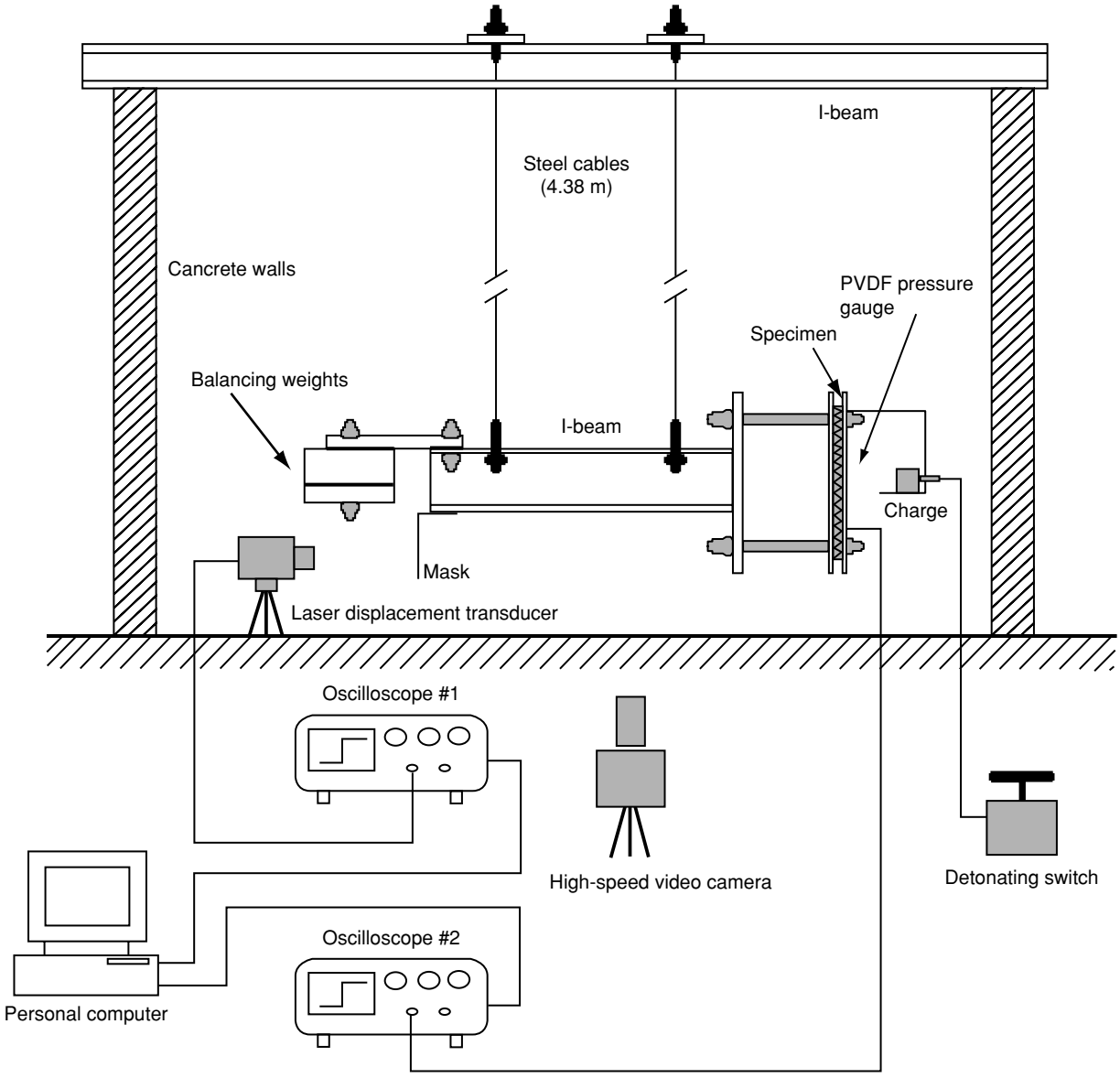

Figure 2. Sketch of the experimental set-up

face to measure the pressure-time history. The complete process of explosion and loading was recorded using a high speed video camera.

2.3. Experimental Results

The experimental results are listed in Table 1. Two types of results are presented and discussed herein, i.e. (1) the deformation/failure patterns observed in the tests, and (2) the quantitative data obtained through measurement and further calculation, e.g. the central point deflection of back face-sheet and impulse transfer. The specimens after tests show that the front face-sheets have attained an inwardly curved dishing deformation, and back face deformed outwardly. The core exhibits a progressive crushing damage, and a cavity between the front face and the crushed foam core was obtained, which is essentially a core fracture, rather than debonding at the interface.

3. SIMULATION

Based on the experiments, a corresponding numerical simulation was conducted using LS-DYNA 970 code, a powerful FEA tool for modeling non-linear mechanics of solids, fluids, gases and their interaction. Based on the explicit numerical methods, LS-DYNA is dedicated to the analysis of dynamic problems associated with large deformation, low and high velocity contact/impact, ballistic penetration and wave propagation, etc.

3.1. FE Model

3.1.1. Modelling geometry

The geometric model of sandwich panel used in the simulations is indicated in Figure 3(a). Due to the symmetric nature of the problem, only a quarter of the panel was modelled. The face-sheets were meshed using the Belytschko-Tsay shell elements (Hallquist 1998), which gives a high computational efficiency, and thus the entire model comprises 6, 050 shells. The foam core was meshed into the eight-node brick (solid) elements, and consists of 90, 750 brick elements.

The explosive charge used in the tests has a cylindrical shape. Eight-node brick (solid) elements with the ALE (Arbitrary Lagrange Euler) formulation (Hallquist 1998) were adopted for the explosive cylinder. The ALE approach uses meshes that are imbedded in material and deform with the material. It combines the best features of both Lagrange and Euler methods, and allows the mesh within any material region to be continuously adjusted in arbitrary and predefined ways as a calculation proceeds, thus providing a continuous and automatic rezoning capability. Therefore, it is very suitable to use an ALE approach to analyse the solid and fluid motions when material strain rate is large and significant, for instance, in the detonation of explosive and volume expansion of explosion products. Figure 3(b) illustrates the geometric model of an explosive cylinder, which consists of 12, 000 solid elements.

3.1.2. Modelling material

The face-sheets of specimens used in the tests were made of aluminium alloy. In the simulations, the mechanical behaviour of aluminium alloy was modelled with the material type 3 (*MAT_PLASTIC_KINEMATIC) in LS-DYNA, which is a bi-linear elasto-plastic constitutive relationship that contains the formulations incorporating isotropic and kinetic hardening. Since aluminium alloy does not show evident strain rate effect, the only input parameters of the material model are: Mass density (ρ), Young's modulus (E), Poisson's ratio (ν), Yield stress (σ_Y) and Tangent modulus (E_{tan}) (Hallquist 1998).

The material type 63 (*MAT_CRUSHABLE_FOAM) in LS-DYNA was used to model the aluminum foams. This is a very simple material model, which allows for a description of the foam behavior through the input of a stress versus volumetric strain curve. The stress versus strain behavior is depicted in Figure 4, which shows an unloading from point **a** to the tension stress cutoff at **b** then unloading to point **c** and finally reloading to point **d**. The input parameters required by this material model are: a material ID, density, Young's modulus, Poisson's

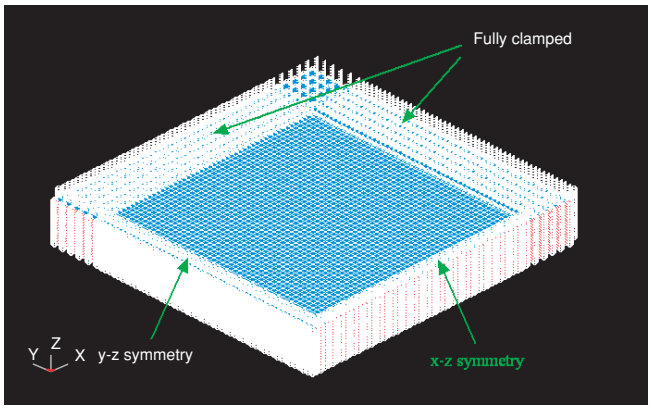

(a) Geometry model of a sandwich panel

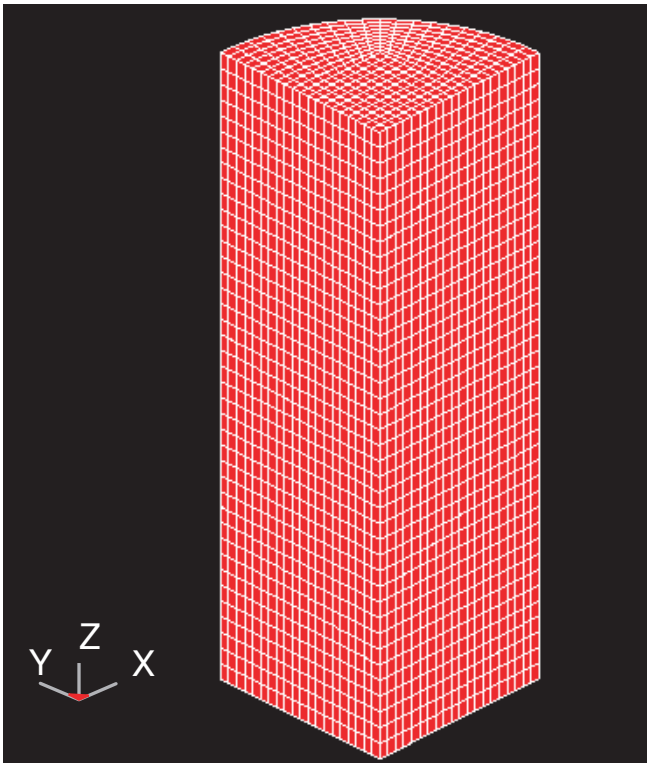

(b) Geometry model of a charge (enlarged view).

Figure 3. Geometric model of a sandwich panel and charge

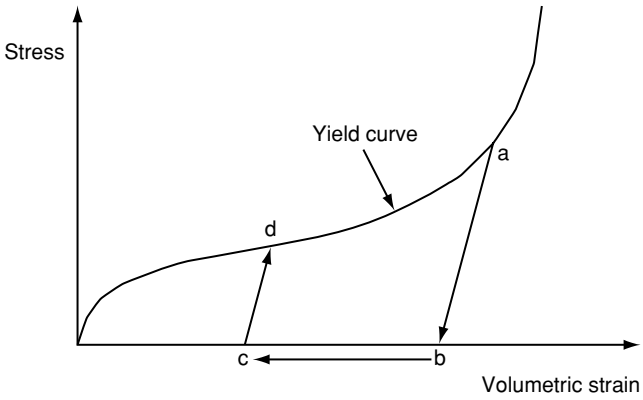

Figure 4. Schematic representation of a stress-strain curve for the material model 63

ratio, a load curve ID, tensile stress cutoff and damping coefficient (Hallquist 1998). In this model, the foam is assumed isotropic and crushed one-dimensionally with a Poisson's ratio that is essentially zero. The model transforms the stresses into the principal stress space where the yielding function is defined, and yielding is governed by the largest principal stress. The principal stresses σ_1, σ_2, σ_3 are compared with the yield stress in compression and tension Y_c and Y_t, respectively. If the actual stress component is compressive, then the stress has to be compared with a yield stress from a given volumetric strain-hardening function specified by the user, $Y_c = Y_c^0 + H(ev)$. On the contrary, when the considered principal stress component is tensile, the comparison with the yield surface is made with regard to a constant tensile cutoff stress $Y_t = Y_t^0$. Hence, the hardening function in tension is similar to that of an elastic, perfectly plastic material (Hanssen *et al*. 2002). Model 63 assumes that the Young's modulus of the foam is constant. The stress-strain curves for the two aluminium foams (6% and 10%) used in this study were from uniaxial compression tests, and are shown in Figure 5. Each curve essentially consists of three stages. At the first stage, the response is linear elastic. This stage terminates when a critical stress is reached and this critical stress level is maintained almost constant over a large range of strain (stage 2). Finally, the stress increases rapidly with strain, as a result of compaction of cells or densification. It can be seen in the figure that the higher relative density leads to a higher plateau stress. The material model 63 was validated under quasi-static compression using the experimental stress-strain curves before applied for the blast loading condition. The stress-strain curves obtained from the numerical simulation are included in Figure 5 as well. The result shows a very good agreement between experiment and computational prediction, and thus indicates that foam behaviour has been accurately characterised by the material model. Subsequent dynamic compression tests showed that the two foams do not have evident strain rate effect.

Since delamination cracks occur in the foam core along a path adjacent to the front face-sheet, the foam core was subdivided such that a thin layer of elements was presented at the interface. The delamination of the foam core was modelled by removing the thin foam interface elements from the mesh, using the material erosion capability of LS-DYNA. Maximum tensile strain (MTS) and maximum shear strain (MSS) were used to define the failure criteria, i.e. any element that has tensile strain greater than MTS or shear strain greater than MSS will fail and be removed from further calculation. Here, it is taken that MTS = 0.2% and MSS = 0.3% (Sriram *et al*. 2006).

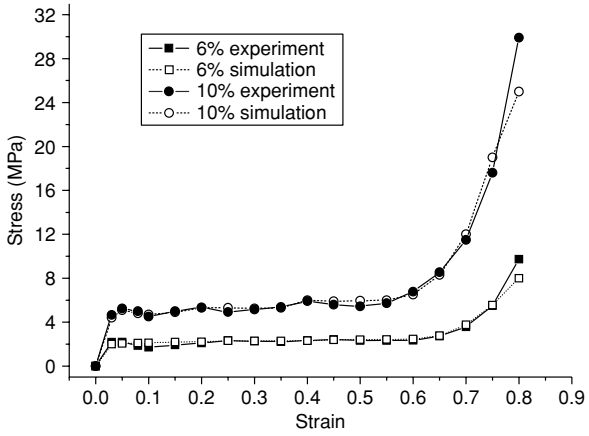

Figure 5. Stress-strain curves of aluminium foams with two relative densities (6% and 10%) obtained from compression test and numerical simulation

The material type 8 (*MAT_HIGH_EXPLOSIVE_BURN) in LS-DYNA was used to describe the material property of the TNT charge. It allows modelling the detonation of a high explosive by three parameters: Mass density of charge (ρ_M), Detonation velocity (V) and Chapman-Jouget pressure (P). Likewise, an equation of state, named Jones-Wilkins-Lee (JWL) equation should be defined with the explosive burn material model. It defines pressure as a function of relative volume, $V^* = \rho_0/\rho$, and internal energy per initial volume, E_{m0}, as

$$P = A\left(1-\frac{\omega\rho}{R_1\rho_0}\right)e^{-R_1\frac{\rho_0}{\rho}} + B\left(1-\frac{\omega\rho}{R_2\rho_0}\right)e^{-R_2\frac{\rho_0}{\rho}} + \frac{\omega\rho}{\rho_0}E_{m0} \quad (1)$$

where P is the blast pressure, ρ is the explosive density, ρ_0 is the explosive density at the beginning of detonation process, A, B, R_1, R_2 and ω are material constants, which are related to the type of explosive and can be found in the explosive handbooks.

Table 2 lists the LS-DYNA material types and mechanical properties of sandwich panel and explosive, and parameters of equations of state (EOS) are also included. The data for face-sheets and core were determined through tensile/compression tests and parameters of explosive were obtained from published literature.

3.1.3. Modelling the blast load

Modelling the blast load on the structure or explosive-structure interaction can be implemented by setting the contact between them (Grobbelaar and Nurick 2000; Mahoi 2006). In this simulation, the load imparted on the front face of sandwich panel was defined with algorithm of *CONTACT_ERODING_SURFACE_TO_

Table 2. LS-DYNA material type, material property and EOS input data

Material	Part	LS-DYNA material type, material property and EOS input data (unit = cm, g, μs)						
Al-2024-T3		*MAT_PLASTIC_KINEMATIC						
	Face sheet	RO	E	PR	SIGY	ETAN		
		2.68	0.72	0.33	3.18E-3	7.37E-3		
Aluminium foam		*MAT_CRUSHABLE_FOAM						
(6%)	Core	RO	E	PR	LCID	TSC	DAMP	
		0.16	7.27E-4	0.0	in Figure 5	2.18E-5	0.1	
Aluminium foam		*MAT_ CRUSHABLE_FOAM						
(10%)	Core	RO	E	PR	LCID	TSC	DAMP	
		0.27	1.55E-3	0.0	in Figure 5	4.66E-5	0.1	
		*MAT_HIGH_EXPLOSIVE_BURN						
		RO	D	PCJ				
		1.63	0.67	0.19				
TNT((Meyer et al.	Charge	*EOS_JWL						
2002)		A	B	R1	R2	OMEG	E0	V0
		3.71	3.23E-2	4.15	0.95	0.30	7.0E-2	1.0

SURFACE, which calculates the interaction between explosion product and structure. The erosion algorithm allows for large distortion of explosion product caused by the reaction of target structure, by eroding elements from its surface contacting the structure.

3.2. Simulation Results and Discussion

The simulation results are reported and discussed in this section, which include three aspects: (1) explosion and structural response process; (2) failure patterns of the sandwich panels observed; and (3) the measured/ calculated quantitative results, which are described in detail in Sections 3.2.1, 3.2.2 and 3.2.3, respectively.

3.2.1. Explosion and structural response process

This sub-section describes a typical process of charge explosion and subsequent plate response, which was calculated by the FE model. The model depicts specimen L-30-TK-1 loaded with a 30g explosive. An entire process consists of three stages:

Stage I – Expansion of the explosive from time of detonation to interaction with the plate
Stage II – Explosive-plate interaction
Stage III – Plate deformation under its own inertia

- Stage I (0~35μs)
  Expansion of explosive starts at the point of detonation (central point of the top surface of charge), and the shock wave created by the detonation compresses and raises the temperature of the explosive at the detonation point of the material, initiating a chemical reaction within a small region just behind the shock wave, known as the reaction zone. Hot gaseous detonation products are produced from the reaction occurring in the reaction zone at the burn speed of the explosive, which is defined in the high explosive material model.

- Stage II (36μs~70μs)
  At this stage, the expanded explosive interacts with the plate front surface. The explosive-plate interaction takes place from approximately t = 36μs to t = 70μs, i.e. over a time period of approximately 35μs, until the contact force between explosive and target structure almost reduces to 0.

  When the contact force between explosive and plate decreases to nearly zero (t = 71μs), their interaction is considered to be finished, and the high explosive model should be manually deleted from the LS-DYNA program. Likewise, to prevent penetration of explosive nodes into the plate, artificial adjustment of contact thickness and contact stiffness is usually necessary.

- Stage III (71μs~5000μs)
  Stage III is the final step of the simulation process, wherein no contact between the explosive is made with the structure, and the plate continues deforming under its own inertia. At this stage, a dent failure is first formed at the central area of sandwich front face, and then deformation extends both outwards and downwards with the transfer of momentum. Likewise, with the development of denting, the thin foam layer adjacent to the front face begins to fail, and delamination occurs between the front face and core. After the deformation zone

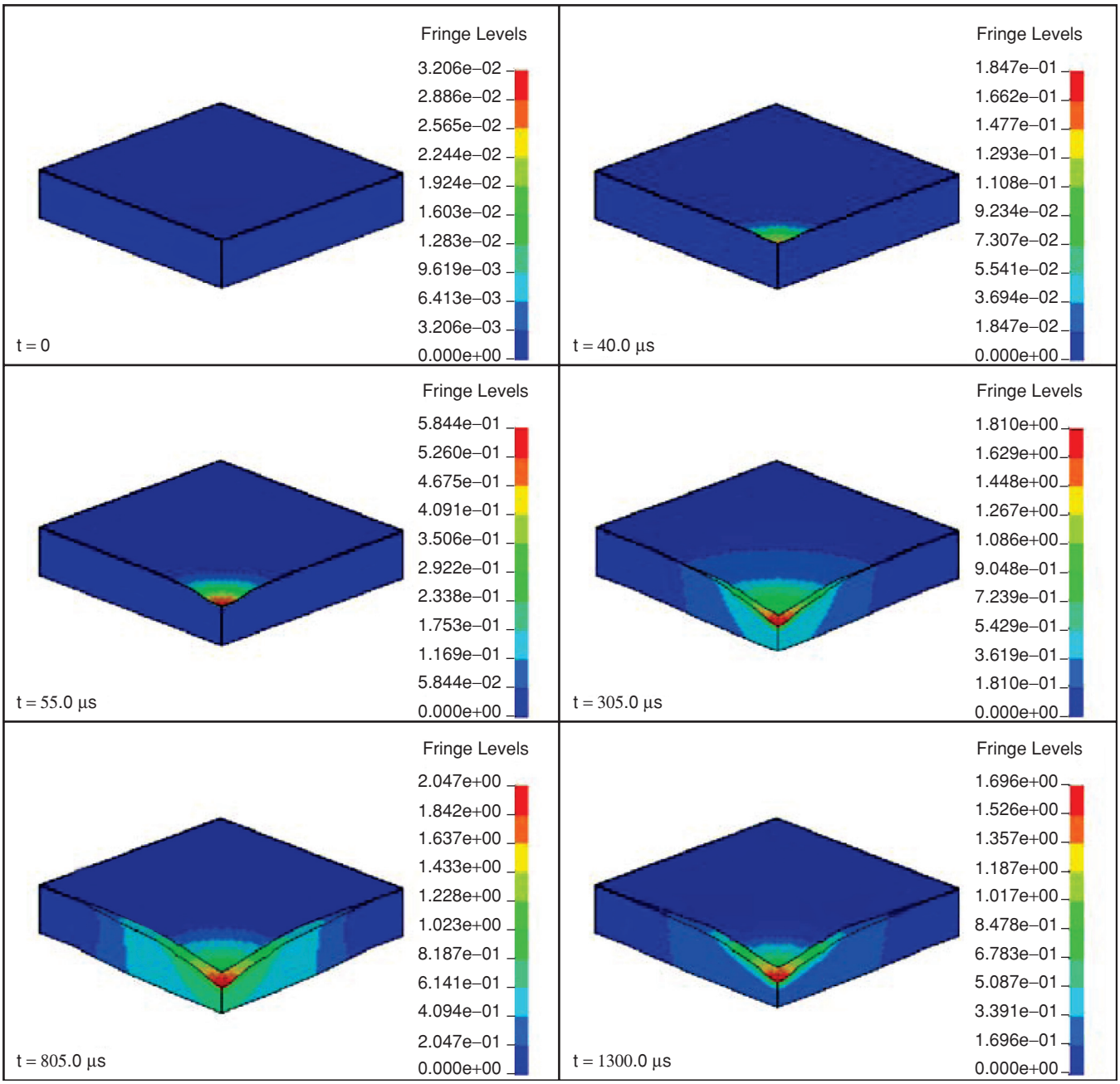

Figure 6. Whole deformation process of a typical panel (Specimen L-30-TK-1)

extends to the external clamped boundaries, a global dishing deformation takes place. A slight oscillation of the plate occurs with the deformation, and the structure is finally brought to rest by plastic bending and stretching. The whole process of the panel deformation (from t = 0) is shown in Figure 6.

3.2.2. Deformation/failure patterns

A typical contour of deformation/failure pattern obtained in the simulation is shown in Figure 7, together with a photograph of a tested specimen. It can be seen that the details of the deformation/failure have been well captured by the simulation. Both face-sheets in the FE model show a typical Mode I response (Jones 1989), which essentially involves a large inelastic deformation, with a denting deformation on the front face and a quadrangular-shaped convexity on the back side. A cavity occurs between the front face and foam core, due to the failure of the thin foam layer adjacent to the front skin. Foam densification can also be observed clearly.

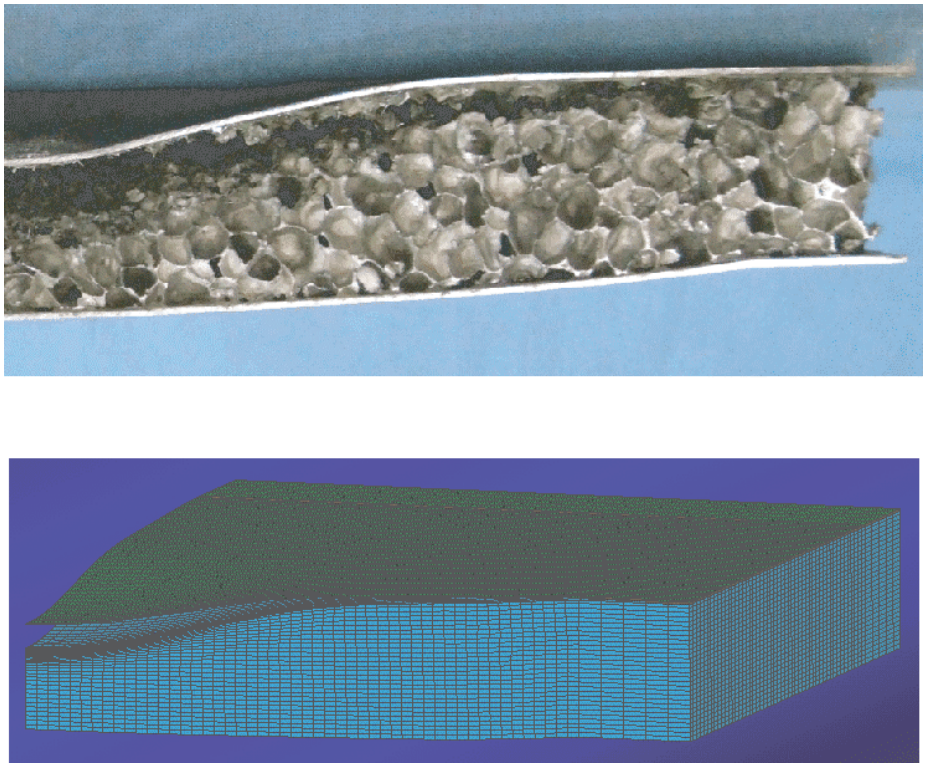

Figure 7. Comparison of the deformation/failure patterns obtained in simulation and experiment (Specimen L-30-TK-1)

3.2.3. Face-sheets deflections and core crushing

The mechanism of deformation/failure is considered as the most important characteristic of structural response as all the other parameters (e.g. impulse transfer and energy absorption in plastic deformation) depend on it. Since people or objects shielded from blast attacks are usually behind sandwich panels, the back face deformation/failure of specimen is herein considered as the main structural response. In this section, a comparison is made between the experiment and simulation results in terms of the final permanent deformation (i.e. deflection) of the central point of back face. A plot of the experimental values versus the predicted values of all the specimens is shown in Figure 8. The data points are very close to the line of perfect match, thus representing a reasonable correlation between the experimental and predicted results.

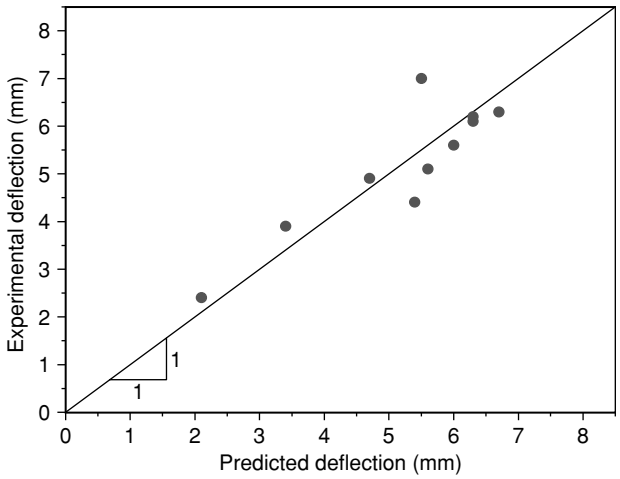

Figure 8. Comparison of predicted and experimental deflections on the back face (Specimen L-30-TK-1)

A typical displacement-time history of the central points of both face-sheets and front surface of the core is illustrated in Figure 9(a). In order to clearly show the details of deformation initiation at the beginning stage, the curves beyond t = 900μs were cut off. It can be observed from the figure that the deformation of the front face and top surface of the core starts at t = 36μs, when the explosion product contacts with the plate, Approximately 55 microseconds later (i.e. t ≈ 90μs), the back face begins to deform, and its deflection increases at a slower pace than the rate at which the front face and front surface of the core deforms. Almost at the same time, delamination between the front face and core takes place, due to the failure of thin foam layer in the interface. After that, the front face-sheet keeps deforming under inertia, at a much slower rate, and reaches its peak at

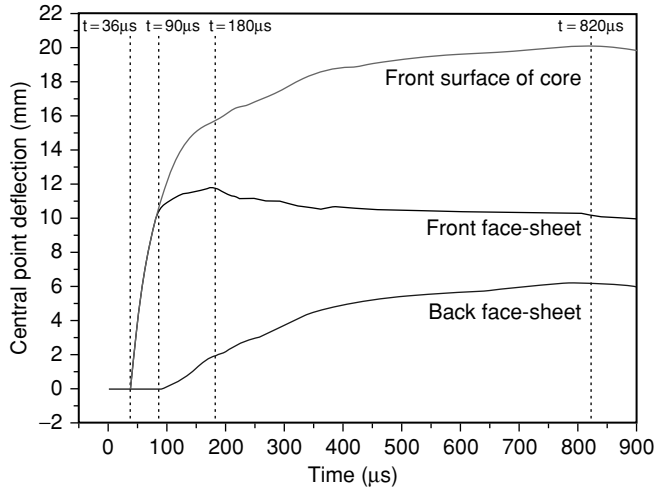

(a) History of central point deflections

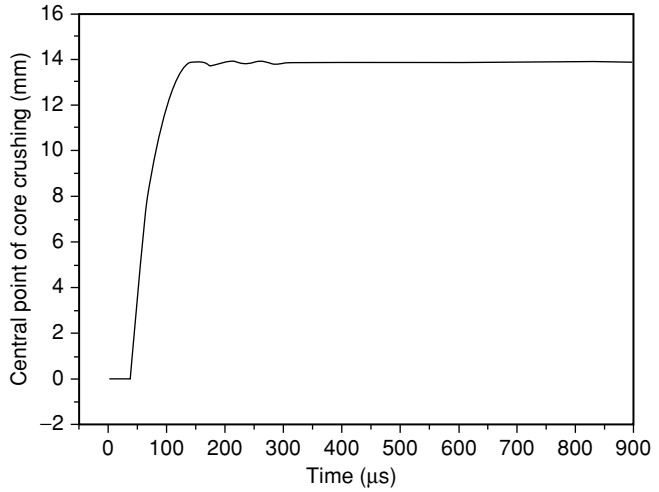

(b) History of core crushing

Figure 9. History of central point deflections and core crushing (Specimen L-30-TK-1)

t ≈ 180μs. On the other hand, the deformation of core and back face continues, until the deflections reach their maximum values at 820μs. Figure 9(b) shows the history of core crushing at the central point.

4. PARAMETRIC STUDY

A parametric study has been conducted to investigate the energy absorbing behaviour of the blast loaded square sandwich panels, which include the time history of plastic dissipation in the face-sheets and core, as well as partition of the plastic energy absorbed by the different component parts of the panels; effect of panel configurations is also analysed.

During the interaction between the explosion product and structure, the explosion energy is transferred to the sandwich panel, and then dissipated by the panel as it deforms. The initial energy transferred to the structure (E_T) is essentially the sum of kinetic (E_K) and internal energy (E_I, also known as deformation energy E_D). The kinetic energy would reduce with time, while the internal energy of the system would increase. Fleck and co-workers theoretically investigated the response of sandwich beams and circular sandwich plates loaded by blasts (Fleck and Deshpande 2004; Qiu *et al*. 2004). The whole deformation has been split into three phases:

Phase I: The blast impulse is delivered onto the front face of sandwich structure, and the front face attains an initial velocity while the rest of the structure is stationary.

Phase II: The core is compressed while the back face is stationary.

Phase III: The back face starts to deform, and the whole structure would deform at the same velocity, and finally the structure is brought to rest by plastic bending and stretching.

Given the impulse delivered on the front face (I), with the impulse transmission, the front face obtains an initial velocity

$$v_0 = \frac{I}{A\rho_f h_f} \tag{2}$$

where A is the exposed area, and ρ_f and h_f are the material density and thickness of face-sheets, respectively. Based on momentum conservation, the kinetic energy of the front face is calculated by Eqn 3, which is the total energy of the structure obtained from the blast load.

$$W_I = \frac{I^2}{2A\rho_f h_f} \tag{3}$$

At the end of Phase II, the whole structure would have the identical velocity, and the kinetic energy can be calculated by

$$W_{II} = \frac{I^2}{2A(2\rho_f h_f + H_c\rho_c)} \tag{4}$$

where ρ_c and H_c are the mass density and thickness of the core, respectively. This part of energy would be dissipated by plastic bending and stretching of the panel in Phase III.

4.1. Time History of Plastic Dissipation

Figure 10 presents a typical time history of the internal energy in each component part of a panel (Specimen L-30-TK-1) during plastic deformation, i.e. front face, back face and core, and the small amount of energy

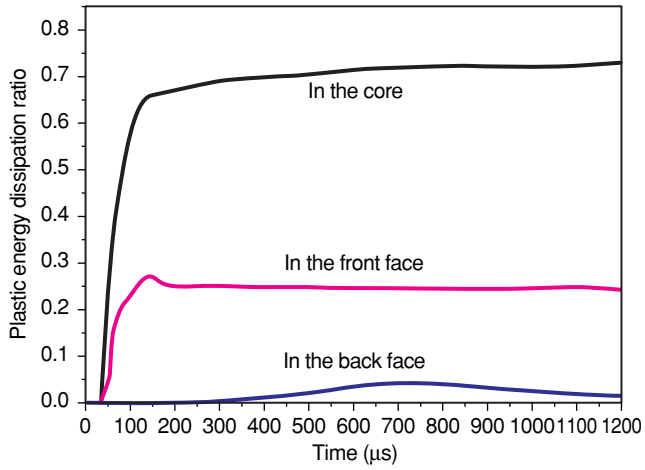

Figure 10. History of plastic dissipation during plastic deformation (Specimen L-30-TK -1)

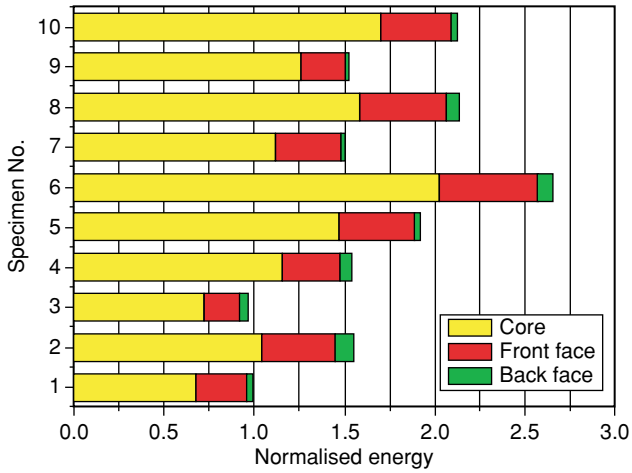

Figure 11. Energy dissipation normalised with the total energy for Specimen No. 1

reduction during the thin layer foam failure in the interface is neglected. The figure shows that in the early stage of the response, lasting until approximately 120μs, the front face sheet flies into the core, resulting in core crushing and significant energy dissipation. After that, the foam core compression almost ceases. From the figure it can be seen that the large deformation of front face and core compression result in significant energy dissipation and core compaction constitutes a major contribution, which is 75% of the total dissipation. Much less energy is absorbed by the back face, as its deformation is maintained at a low level.

4.2. Energy Partition

The partition of the energy absorbed by different parts of the panels during deformation is indicated in a stack bar diagram in Figure 11. Using the plastic energy absorption in Specimen No. 1 as a benchmark, the plastic dissipations by the other nine plates are expressed in a normalised form with the total energy absorbed by the first panel. Their energy dissipation is compared and analysed in terms of (1) impulse level, (2) relative density of core, (3) face-sheet thickness and (4) core thickness.

4.2.1. Effect of impulse level

In order to study the performance of the panels at different levels of blast loading, all the ten panels are divided into five groups, i.e. 1 & 2, 3 & 4, 5 & 6, 7 & 8 and 9 & 10, and in each group, the two panels have an identical configurations but loaded by charges with different masses. Increasing impulse levels by 23.4%~27.0% (for 1 & 2 and 3 & 4) and 14.3%~15.8% (for the rest) leads to a rise of total internal energy dissipation in the panels. The increases in internal energy in each group are 53.8%, 60.4%, 37.8%, 41.5%, and 34.8%, respectively, which are close to the results obtained from Eqn 3 that the total energy input (W_I) is proportional to the square of the total impulse input (I^2).

4.2.2. Effect of face-sheet thickness

Four specimens have been selected and grouped as two pairs (i.e. 5 & 7 and 6 & 8) to investigate the effect of face-sheet thickness on their energy absorbing performance. It is evident that at two levels of impulse, compared with the panels with thicker face-sheets (1mm) the internal energy in those with thinner faces (0.8mm) increases significantly, i.e. by 31.6% and 28.0% respectively. Eqn 3 indicates that the 0.8mm skin would lead to a 25% increase in the total energy, which is close to the simulation result obtained. Therefore, it is concluded that a sandwich panel with thinner face-sheets can improve its energy absorbing capability. However, when under large blast loading, tearing damage may take place on the thinner front face (e.g. Specimen 6 (L-30-MD-2)).

4.2.3. Effect of relative density of core

Effect of relative density of core has been analysed by taking eight panels, which are divided into four groups: 1 & 3, 2 & 4, 7 & 9 and 8 &10, respectively. Specimens 1, 2, 7 and 9 have low density cores (6%) while the cores in the other panels are of high density (10%). The simulation result shows that all the four groups exhibit a similar trend. The total internal energy for the panels with different core densities in each group is very close, but the contribution of core in Specimens 3, 4, 9 and 10 increases by 7.0%, 8.0%, 8.0% and 5.9% respectively, compared with in Specimens 1, 2, 7 and 8. Therefore one can conclude that the portion of energy absorption by the core can be increased by increasing its density.

4.2.4. Effect of core thickness

Four panels have been grouped as Specimens 2 & 7 and 4 & 9. Each group has a single core thickness, i.e. 200mm and 300mm respectively. The simulation result shows that the total dissipations by the four panels are very similar. Compared with Specimens 2 and 4, in Panels 7 and 9, the percentages of the dissipation by the back faces, reduce from 6.3% to 1.3% and 3.9% to 0.9%, respectively. This is because in the panels with a thicker core, back faces have smaller deflections, and thus less energy is dissipated.

5. CONCLUSIONS

Experimental investigations have been carried out to study the resistant behaviour and energy absorbing performance of square sandwich panels under blast loading. Based on the experiments, a corresponding numerical simulation study has been conducted using LS-DYNA software.

In the simulation, a crushable foam constitutive relationship has been used to model the material property of aluminium foam. A thin layer of foam was set with a failure criterion in the interface of front face and core to simulate the delamination crack by removing the failed elements. The TNT charge has been meshed using solid elements with the ALE formulation. Its mechanical behaviour is governed by a high explosive material model incorporating the JWL equation of state. The process of charge explosion and plate response was simulated with three stages, that is, Stage I – Expansion of the explosive from time of detonation to interaction with the plate; Stage II – Explosive plate interaction; and Stage III – Plate deformation under its own inertia. The FE model predicts similar deformation/failure patterns as observed experimentally for both face-sheets and core structure. Likewise, the simulation results demonstrate a reasonable agreement with the measured quantitative data obtained in the experiment. Finally, a parametric study was conduced to analyse the energy absorption in each part during plastic deformation. It is concluded that the foam core constitutes a major contribution to energy dissipation; thinner face-sheets can raise the total internal energy; while denser and thicker core can increase its portion of energy dissipation.

Analytical model for such square panels under blasts has been developed and reported in a separated paper (Zhu et al. 2009).

ACKNOWLEDGEMENTS

The reported research is financially supported by the Australian Research Council (ARC) through a Discovery Grant and China Natural Science Funding under the number of 10572100 and 90716005, which are gratefully acknowledged.

The authors would like to thank the academic and technical staff members at North University of China involved in this project, for their provision of experimental facilities and technical assistance; and thank the Victorian Partnership for Advanced Computing (VPAC), Australia for the access to their high performance computing facilities. They also thank Professor E. Gad for helpful discussions.

REFERENCES

Ashby, M.F., Evans, A.G., Fleck, N.A., Gibson, L.J., Hutchinson, J.W. and Wadley, H.N.G. (2000). *Metal Foams: A Design Guide*, Cambridge University Press, New York, USA.

Fleck, N.A. and Deshpande, V.S. (2004). "The resistance of clamped sandwich beams to shock loading", *Journal of Applied Mechanics,* ASME, Vol. 71, pp. 1–16.

Gibson, L.J. and Ashby, M.F. (1997) *Cellular Solids: Structure and Properties,* 2nd edition, Cambridge University Press, Cambridge, UK.

Grobbelaar, W.P. and Nurick, G.N. (2000). "An investigation of structures subjected to blast loads incorporating an equation of state to model the material behaviour of the explosive", *Proceedings of the 7th International Symposium on Structural Failure and Plasticity (IMPLAST2000)*, Melbourne, Australia, pp. 185–194.

Hallquist, J.O. (1998). *LS-DYNA Theoretical Manual*, Livermore Software Technology Co., Livermore, CA, USA.

Hanssen, A.G., Hopperstad, O.S., Langseth, M. and Ilstad, H. (2002). "Validation of constitutive models applicable to aluminium foams", *International Journal of Mechanical Sciences*, Vol. 44, No. 2, pp. 359–406.

Jones, N. (1989). *Structural Impact*, Cambridge University Press, Cambridge, UK.

Lu, G. and Yu, T.X. (2003). *Energy Absorption of Structures and Materials*, Woodhead Publishing Ltd., Cambridge, UK.

Mahoi, S. (2006). *Influence of Shape of Solid Explosives on the Deformation of Circular Steel Plates – Experimental and Numerical Investigations*, PhD Thesis, University of Cape Town, Cape Town, South Africa.

Meyer, R., Köhler, J. and Homburg, A. (2002). *Explosives,* 5th edition, Wiley-VCH, Weinheim, Germany.

Qiu, X., Deshpande, V.S. and Fleck, N.A. (2003). "Finite element analysis of the dynamic response of clamped sandwich beams subject to shock loading", *European Journal of Mechanics A/Solids*, Vol. 22, No. 6, pp. 801–814.

Qiu, X., Deshpande, V.S. and Fleck, N.A. (2004). "Dynamic response of clamped circular sandwich plate subject to shock loading", *Journal of Applied Mechanics*, ASME, Vol. 71, No. 5, pp. 637–645.

Sriram, R., Vaidya, U.K. and Kim, J.E. (2006). "Blast impact response of aluminum foam sandwich composites", *Journal of Material Science*, Vol. 41, No. 13, pp. 4023–4039.

Xue, Z. and Hutchinson, J.W. (2003). "Preliminary assessment of sandwich plates subject to blast loading", *International Journal of Mechanical Sciences*, Vol. 45, pp 687–705.

Zhu F., Zhao L.M,. Lu G. and Wang Z. (2008). "Deformation and failure of impulsive loaded metallic sandwich panels – Experimental investigations", *International Journal of Impact Engineering*, Vol. 35, pp.937-951.

Zhu F., Wang Z., Lu G. and Zhao L.M. (2009). "Analytical investigation and optimal design of sandwich panels subjected to shock loading", *Materials & Design*, Vol. 30, pp. 91-100.